Published by :
https://www.ijert.org/
An International Peer-Reviewed Journal

International Journal of Engineering Research & Technology (IJERT)
ISSN: 2278-0181
Vol. 15 Issue 05 , May - 2026

Day-Ahead Scheduling of Cool Thermal Energy Storage for PV-Supported Hot-Climate Systems

Dr. Hisham Alharbi
Department of Electrical Engineering, College of Engineering, Taif University, Taif 21944, Saudi Arabia.

***Abstract*—This paper presents a compact day-ahead scheduling framework for a system with Photovoltaic (PV) generation, cooling demand, battery energy storage, and cool thermal energy storage (CTES) in a hot-climate setting. The proposed mixed-integer linear programming model schedules grid import, chiller, battery, and CTES operation under time-of-use electricity pricing and a grid-import constraint. Four storage configurations are evaluated: no storage, battery-only storage, CTES-only storage, and hybrid battery-CTES storage. The results show that the no-storage case has the highest daily operating cost because the grid-import limit causes some load shedding. In contrast, all storage configurations eliminate load shedding and reduce the operating cost by approximately 28%. Among the tested configurations, the CTES-only case achieves the lowest operating cost, reflecting the value of cooling-side storage in hot climates. The hybrid case provides a balanced flexibility structure by combining electrical support from the battery and cooling-side shifting from CTES. The results highlight the different operational roles of electrical and cooling storage in PV-supported hot-climate systems.**

***Index Terms*—PV-supported grids, hot-climate cooling, cool thermal energy storage, battery energy storage, time-of-use pricing.**

I. Introduction

THE rapid growth of cooling electricity demand is one of the main challenges facing energy systems in hot-climate regions. In Saudi Arabia, air-conditioning represents a major contributor to residential and commercial electricity use, particularly during summer periods when high ambient temperatures coincide with system peak demand [1]–[3]. At the same time, the increasing deployment of on-site photovoltaic (PV) generation provides an opportunity to supply part of the daytime cooling demand locally within microgrids. These conditions make cooling loads a suitable target for operational flexibility, especially in grids where PV generation, cooling demand, and electricity prices vary over the day. However, the timing of PV production, cooling demand, and high tariff grid electricity is not always identical. Therefore, energy storage can be used to shift energy use, support operation under grid-import constraints, reduce reliance on high tariff grid electricity, and improve the economic performance of grid-connected microgrids.

Battery energy storage systems are commonly considered for systems with PV generation because they can store excess electricity and discharge it later. They are flexible and can support PV self-consumption, peak shaving, and energy arbitrage [4]. However, when a large portion of the grid demand is associated with cooling, flexibility does not necessarily have to be provided only through electrical storage. In this case, energy can also be stored in the form of useful cooling. Particularly, cool thermal energy storage (CTES), including chilled-water or ice-based storage, stores useful cooling directly and can therefore shift chiller operation from high-tariff or high-demand periods to periods with lower grid prices or higher PV availability [5], [6]. This introduces a different storage pathway in which the cooling demand itself becomes part of the scheduling problem.

At a broader system level, thermal storage has also been examined in renewable energy communities and integrated building energy systems [7], [8]. In these applications, thermal storage is treated as part of coordinated energy management rather than only as an auxiliary cooling component. This wider perspective is important because it connects thermal storage operation with renewable generation, electricity prices, and demand-side scheduling.

Following this broader discussion, several studies have investigated optimal operation and control of ice-storage and cool-storage systems. Candanedo et al. [9] studied model-based predictive control of an ice storage device in a building cooling system, showing the value of using predictive information to schedule storage charging and discharging rather than relying only on fixed control rules. This is important because CTES operation is strongly time-coupled, where charging decisions made during low-cost or high-PV periods affect the ability to satisfy cooling demand later in the day. In addition, chiller efficiency can vary with operating conditions, including part-load operation, which further affects the value of shifting cooling production over time [10]. Vetterli and Benz [6] presented a cost-optimal design of an ice-storage cooling system using mixed integer linear programming (MILP) under different electricity tariff schemes. At the community scale, Heine et al. [11] proposed a simulation-optimization workflow for packaged ice storage systems within a connected community to determine storage design and dispatch decisions.

Recent work has continued to extend the modeling of CTES under practical operating conditions. Tu et al. [12] studied optimal operation of ice-storage air-conditioning systems while considering thermal comfort and demand response. The proposed formulation included TOU price structures and comfort-related constraints, which highlights that cooling-storage scheduling should not be evaluated only from the electricity-cost side. Hillen et al. [13] proposed a MILP framework for seasonal ice-storage operation with time-series aggregation, including physical features such as sensible and latent storage behavior.

Other studies have examined the coordination of electrical and thermal flexibility in buildings. Niu et al. [14] studied

Hisham Alharbi is with the Department of Electrical Engineering, College of Engineering, Taif University, Taif 21944, Saudi Arabia.
Corresponding author: Hisham Alharbi, e-mail: h.alharbi@tu.edu.sa.

International Journal of Engineering Research & Technology (IJERT)
ISSN: 2278-0181
Vol. 15 Issue 05 , May - 2026

flexible dispatch of an energy system using both thermal storage and battery energy storage. Their results indicate that economic dispatch can reduce operating cost, but the optimization objective can also affect the feeder power profile. Rostamnezhad et al. [15] proposed an electricity-consumption optimization framework using thermal and battery energy storage systems. The results show that electrical and thermal storage can provide complementary flexibility. These findings indicate that batteries and thermal storage may provide different forms of flexibility in grid operation.

A related group of studies adds air-conditioning and building-cooling operation to the battery-thermal storage coordination problem. Shakir et al. [16] investigated coordinated optimization of household air conditioning and battery energy storage under TOU pricing, showing that battery operation can be coordinated with cooling loads to improve energy management. Kang et al. [17] studied a PV-integrated building cooling system with electricity storage and ice storage under source-load uncertainties. These studies demonstrate the importance of coordinating storage operation with air-conditioning and building-cooling demand. However, they do not provide a direct comparison of battery-only, CTES-only, and hybrid storage configurations under the same PV profile, tariff structure, cooling-demand pattern, and grid operating limits.

The need for this comparison is particularly important in hot-climate microgrids, where cooling is not a secondary load but one of the main drivers of electricity demand and peak hours. In Saudi Arabia, previous studies have emphasized the large impact of air-conditioning on electricity demand and the need for cooling-related demand-side flexibility [2], [3]. This point is further supported by recent studies on efficient residential cooling systems, future residential electricity demand, and PCM-assisted air-conditioning under Riyadh climatic conditions [18]–[20]. When cooling demand has this role, battery storage and CTES affect operation through different pathways: a battery can shift PV-generated electricity and support the electrical load directly, whereas CTES shifts cooling production and reduces chiller electricity use during constrained or high-tariff hours. Therefore, the hot-climate context motivates the comparison of battery and cooling-storage operation in PV-supported microgrids.

The above studies provide useful models for CTES, battery storage, air-conditioning operation, and thermal flexibility. However, a remaining gap is the direct comparison of battery storage and CTES in a PV-supported grid-connected microgrid under the same operating conditions. In particular, the literature often focuses either on battery-based electrical storage, cooling-storage control, or broader integrated energy-system formulations. Fewer studies use a simple case-study structure to separate the operational roles of battery-only, CTES-only, and hybrid storage configurations. This distinction is important because the two storage pathways interact differently with grid-constrained operation, tariff-responsive scheduling, chiller loading, and non-cooling load-shedding mitigation. Accordingly, the gap addressed in this paper is the comparison of these storage configurations under a common operating framework that makes their operational roles easier to interpret.

To address this gap, this paper develops a compact day-ahead scheduling framework for a PV-supported hot-climate microgrid with cooling demand, battery storage, and CTES. The framework represents the main electrical and cooling-side decisions, including grid import, PV use, chiller scheduling, and storage charging and discharging, while accounting for TOU pricing and the grid-import limit. Rather than treating storage as a single flexibility source, the model is used to compare how battery storage and CTES affect the operation of a cooling-dominated microgrid through different pathways. The case-study analysis considers no-storage, battery-only, CTES-only, and hybrid battery-CTES configurations under one consistent operating setup. This allows the differences in cost, grid-constrained operation, and cooling-side shifting to be attributed to the available storage technology.

The main contributions of this paper are summarized as follows:

- A compact MILP day-ahead scheduling model is developed for a grid-connected microgrid that integrates PV generation, battery storage, and cool thermal energy storage to serve electrical and cooling demand in a hot-climate setting.
- The storage configurations are compared under the same TOU tariff, PV profile, non-cooling electrical demand, and cooling-demand profile to evaluate battery-only, CTES-only, and hybrid battery-CTES storage operation.
- The results clarify the different operational roles of battery storage and CTES in reducing operating cost, managing grid-import limits, and shifting cooling-related demand.

The remainder of this paper is organized as follows: Section II presents the proposed day-ahead scheduling model and its main operating constraints. Section III describes the test system and input data. Section IV presents the case studies and discusses the simulation results. Section V concludes the paper.

II. Proposed PV-supported Cooling Storage Scheduling Framework

A. Problem Description and Modeling Framework

This paper considers the day-ahead operation of a grid-connected, PV-supported hot-climate microgrid with non-cooling electrical demand, cooling demand, battery energy storage, and CTES. The model is formulated for a cooling-dominated application in which these resources are coordinated under TOU electricity pricing and a grid-import limit.

The proposed framework is developed as a unified MILP scheduling model. PV generation can supply the electrical demand, the chiller, or battery charging demand. Since grid export is not considered, unused PV generation is curtailed. The battery provides electrical flexibility by charging and discharging within the electrical balance, while the CTES provides cooling-side flexibility by storing cooling produced by the chiller and discharging it to reduce chiller operation during peak price or grid-constrained hours.

International Journal of Engineering Research & Technology (IJERT)
ISSN: 2278-0181
Vol. 15 Issue 05 , May - 2026

The scheduling problem is formulated over a 24-h horizon with hourly intervals. The objective is to minimize the daily operating cost, including electricity purchase cost, PV curtailment penalty, and electrical load-shedding penalty. Cooling demand is treated as mandatory, hence no unmet-cooling is considered. A limited amount of electrical load shedding is allowed but penalized with a high cost coefficient, so it is used only when the available supply and storage resources are insufficient.

The main decision variables include grid import P_t^{Grid}, utilized PV power P_t^{PV}, curtailed PV power P_t^{Curt}, non-cooling electrical load shedding P_t^{Shed}, chiller electrical input P_t^{Ch}, chiller cooling output $Q_t^{Ch,out}$, direct cooling supply Q_t^{Dir}, battery charging and discharging powers $P_t^{Bat,ch}$ and $P_t^{Bat,dis}$, battery stored energy E_t^{Bat}, CTES charging and discharging rates $Q_t^{CTS,ch}$ and $Q_t^{CTS,dis}$, and stored cooling energy E_t^{CTS}.

B. Objective Function

The objective function is to minimize the day-ahead operating cost C^{Op}, as follows:

$$C^{Op} = \sum_{t\in\mathcal{T}} \left[\rho_t P_t^{Grid} + C^{Curt} P_t^{Curt} + C^{Shed} P_t^{Shed}\right] \Delta t. \tag{1}$$

where ρ_t is the time-of-use (TOU) electricity purchase tariff, C^{Curt} is the PV-curtailment penalty coefficient, C^{Shed} is the penalty coefficient for non-cooling electrical load shedding, and Δt is the scheduling time step.

C. Electrical Power Balance and PV Allocation

The hourly electrical power balance is written as

$$P_t^{Grid} + P_t^{PV} + P_t^{Bat,dis} + P_t^{Shed} = P_t^{Base} + P_t^{Ch} + P_t^{Bat,ch}, \quad \forall t \in \mathcal{T}. \tag{2}$$

where P_t^{Base} is the exogenous non-cooling electrical demand and P_t^{Ch} is the electrical input power of the chiller. The load shedding cannot exceed the available base load in each hour, as follows:

$$0 \le P_t^{Shed} \le P_t^{Base}, \quad \forall t \in \mathcal{T}. \tag{3}$$

The available PV generation is either utilized locally or curtailed, as follows:

$$P_t^{PV} + P_t^{Curt} = \overline{P}_t^{PV}, \quad \forall t \in \mathcal{T}. \tag{4}$$

$$P_t^{PV} \ge 0, \quad P_t^{Curt} \ge 0, \quad \forall t \in \mathcal{T}. \tag{5}$$

The grid import is bounded by the microgrid interconnection limit:

$$0 \le P_t^{Grid} \le P^{Grid,\max}, \quad \forall t \in \mathcal{T}. \tag{6}$$

D. Electric Chiller and Cooling Balance

The electric chiller converts electrical input power into cooling output according to an hourly coefficient of performance:

$$Q_t^{Ch,out} = \mathrm{COP}_t^{Ch} P_t^{Ch}, \quad \forall t \in \mathcal{T}. \tag{7}$$

where COP_t^{Ch} is the exogenous hourly chiller coefficient of performance. This hourly profile is used to represent the variation in chiller performance over the day due to changing operating and ambient-temperature conditions.

The chiller electrical input is bounded by its rated capacity:

$$0 \le P_t^{Ch} \le P^{Ch,\max}, \quad \forall t \in \mathcal{T}. \tag{8}$$

The chiller cooling output is divided between direct cooling supply and CTES charging, while the cooling demand is supplied by direct chiller output and CTES discharge, as follows:

$$Q_t^{Ch,out} = Q_t^{Dir} + Q_t^{CTS,ch}, \quad \forall t \in \mathcal{T}. \tag{9}$$

$$Q_t^{Cool} = Q_t^{Dir} + Q_t^{CTS,dis}, \quad \forall t \in \mathcal{T}. \tag{10}$$

where Q_t^{Cool} is the exogenous cooling demand. This balance enforces full cooling-demand supply in each hour. Therefore, the model does not introduce an unmet-cooling variable or a separate thermal-discomfort penalty.

E. Battery Energy Storage Model

The battery state of charge is represented by the stored electrical energy E_t^{Bat}. The battery energy balance is given by

$$E_t^{Bat} = (1-\lambda^{Bat})E_{t-1}^{Bat} + \eta^{Bat,ch} P_t^{Bat,ch} \Delta t - \frac{P_t^{Bat,dis}}{\eta^{Bat,dis}} \Delta t, \quad \forall t \in \mathcal{T}. \tag{11}$$

where λ^{Bat} is the hourly battery self-discharge coefficient, and $\eta^{Bat,ch}$ and $\eta^{Bat,dis}$ are the battery charging and discharging efficiencies, respectively.

The initial battery state is fixed as a fraction of the installed battery capacity, and the terminal battery state is also fixed to preserve comparable operation across the daily scheduling horizon:

$$E_0^{Bat} = \mathrm{SOC}^{Bat,ini} E^{Bat,\max}. \tag{12}$$

$$E_T^{Bat} = \mathrm{SOC}^{Bat,ref} E^{Bat,\max}. \tag{13}$$

The battery stored energy is bounded by its installed capacity, and the battery charging and discharging powers are limited as follows:

$$0 \le E_t^{Bat} \le E^{Bat,\max}, \quad \forall t \in \mathcal{T}. \tag{14}$$

$$0 \le P_t^{Bat,ch} \le P^{Bat,ch,\max} u_t^{Bat,ch}, \quad \forall t \in \mathcal{T}, \tag{15}$$

$$0 \le P_t^{Bat,dis} \le P^{Bat,dis,\max} u_t^{Bat,dis}, \quad \forall t \in \mathcal{T}. \tag{16}$$

To prevent simultaneous charging and discharging, the battery operating modes are constrained by

$$u_t^{Bat,ch} + u_t^{Bat,dis} \le 1, \quad \forall t \in \mathcal{T}. \tag{17}$$

where $u_t^{Bat,ch}$ and $u_t^{Bat,dis}$ are binary variables indicating the charging and discharging modes of the battery. In cases without battery storage, $E^{Bat,\max}$, $P^{Bat,ch,\max}$, and $P^{Bat,dis,\max}$ are set to zero.

International Journal of Engineering Research & Technology (IJERT)
ISSN: 2278-0181
Vol. 15 Issue 05 , May - 2026

F. Cool Thermal Energy Storage Model

The CTES state of charge is represented by the stored cooling energy E_t^{CTS}. The CTES energy balance is written as

$$E_t^{CTS} = (1-\lambda^{CTS})E_{t-1}^{CTS} + \eta^{CTS,ch}Q_t^{CTS,ch}\Delta t - \frac{Q_t^{CTS,dis}}{\eta^{CTS,dis}}\Delta t, \forall t \in \mathcal{T}. \quad (18)$$

where λ^{CTS} is the hourly thermal loss coefficient, and $\eta^{CTS,ch}$ and $\eta^{CTS,dis}$ are the CTES charging and discharging efficiencies, respectively.

The initial and terminal CTES state is fixed as a fraction of the installed CTES capacity, as follows:

$$E_0^{CTS} = \mathrm{SOC}^{CTS,ini}E^{CTS,\max}. \quad (19)$$

$$E_T^{CTS} = \mathrm{SOC}^{CTS,ref}E^{CTS,\max}. \quad (20)$$

The stored cooling energy is bounded by the installed CTES capacity, while the CTES charging and discharging rates are limited as follows:

$$0 \le E_t^{CTS} \le E^{CTS,\max}, \quad \forall t \in \mathcal{T}. \quad (21)$$

$$0 \le Q_t^{CTS,ch} \le Q^{CTS,ch,\max}u_t^{CTS,ch}, \quad \forall t \in \mathcal{T}, \quad (22)$$

$$0 \le Q_t^{CTS,dis} \le Q^{CTS,dis,\max}u_t^{CTS,dis}, \quad \forall t \in \mathcal{T}. \quad (23)$$

To prevent simultaneous CTES charging and discharging, the CTES operating modes are constrained by

$$u_t^{CTS,ch} + u_t^{CTS,dis} \le 1, \quad \forall t \in \mathcal{T}. \quad (24)$$

where $u_t^{CTS,ch}$ and $u_t^{CTS,dis}$ are binary variables indicating the CTES charging and discharging modes, respectively. In cases without CTES, $E^{CTS,\max}$, $Q^{CTS,ch,\max}$, and $Q^{CTS,dis,\max}$ are set to zero.

This proposed formulation is a MILP model because it combines linear operational constraints with binary variables for storage operating modes and grid-constrained scheduling decisions. This structure enables the day-ahead operation of the PV-supported cooling microgrid to be optimized while preserving computational tractability.

III. Test System and Model Parameters

The proposed PV-supported Cooling Storage Scheduling Framework is implemented in GAMS and solved using CPLEX. The test system represents a grid-connected campus cooling microgrid in a hot climate setting. It consists of non-cooling electrical demand, on-site PV generation, utility grid import, an electric chiller, battery energy storage, CTES, and cooling demand. The scheduling horizon is 24 h with hourly resolution. Grid export is not considered, and PV curtailment is allowed when the available PV generation cannot be utilized by the electrical load, the chiller, or the storage devices.

The exogenous 24-hour profiles of non-cooling electrical demand, available PV generation, and cooling demand are shown in Fig. 1. The cooling-demand profile is selected to represent a hot-climate daily pattern, where the cooling requirement increases during the daytime and overlaps with the reported summer peak-demand interval in Saudi Arabia.

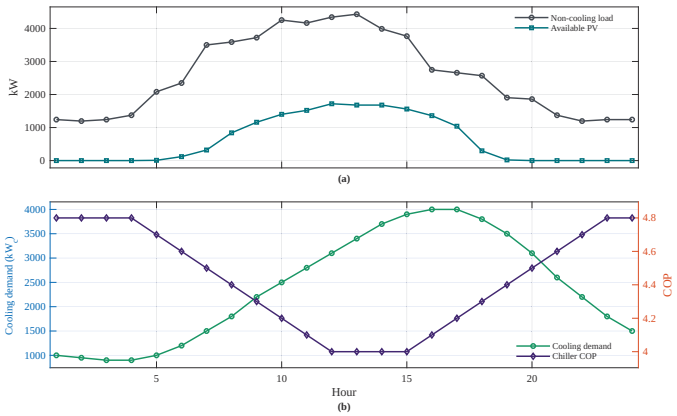

Fig. 1. Input profiles used in all case studies: (a) electrical load and PV generation, and (b) cooling demand and chiller COP over the 24-h scheduling horizon.

The electricity purchase tariff follows a representative TOU structure. The off-peak electricity price is set to 0.085 \$/kWh, while the peak-period price is set to 0.30 \$/kWh during hours 11-17. The grid import limit is set to $P^{Grid,\max} = 3400$ kW. The TOU tariff is used as a scenario input to evaluate tariff-responsive operation under a constrained grid-connection condition, motivated by previous Saudi studies on TOU pricing and demand-side response [21], [22].

Cooling demand is treated as a mandatory demand in the scheduling problem, and no unmet-cooling variable is introduced. The non-cooling electrical demand is also prioritized, but a limited load-shedding variable is included. This variable is penalized by $C^{Shed} = 10$ \$/kWh in the objective function, so load shedding is used only when the available supply and storage resources are insufficient to fully serve the electrical demand. The PV-curtailment penalty is set to $C^{Curt} = 0.001$ \$/kWh to discourage unnecessary curtailment when storage or load-shifting options are available. The hourly self-discharge coefficient of the battery and the hourly thermal loss coefficient of the CTES are both set to zero in this test system.

The electric chiller, CTES, and battery energy storage parameters are summarized in Table I. The maximum chiller electrical input is set to 1000 kW. An hourly COP profile is adopted, with values ranging from 4.0 during the hottest daytime hours to 4.8 during the lower-temperature hours, as shown in Fig. 1(b). This profile represents the variation of chiller efficiency over the day rather than assuming a single fixed COP [10]. The storage capacities, power ratings, charging/discharging efficiencies, and initial and terminal stored-energy fractions are listed in Table I. The initial and terminal storage levels are fixed at 50% to preserve comparable daily operating conditions.

The storage ratings are selected using a nominal electrical-equivalent normalization based on a reference chiller COP of $\mathrm{COP}^{Ch,ref} = 4.0$. Under this reference value, 1000 kWh of electrical storage corresponds to approximately 4000 kWh$_c$ of cooling production, and a 500 kW electrical shifting capability corresponds to approximately 2000 kW$_c$ of cooling capacity. This normalization provides a transparent size ba-

International Journal of Engineering Research & Technology (IJERT)
ISSN: 2278-0181
Vol. 15 Issue 05 , May - 2026

TABLE I
ELECTRIC CHILLER, CTES, AND BATTERY ENERGY STORAGE PARAMETERS ADOPTED IN THE TEST SYSTEM.

Component	Parameter	Value	Unit
Electric chiller	$P^{Ch,\max}$	1000	kW
	COP_t^{Ch}	4.0–4.8	–
	$\mathrm{COP}^{Ch,ref}$	4.0	–
CTES	$E^{CTS,\max}$	4000	kWh_c
	$Q^{CTS,ch,\max}$	2000	kW_c
	$Q^{CTS,dis,\max}$	2000	kW_c
	$\eta^{CTS,ch}$	0.95	–
	$\eta^{CTS,dis}$	0.95	–
	$\mathrm{SOC}^{CTS,ini}$	0.50	–
	$\mathrm{SOC}^{CTS,ref}$	0.50	–
Battery energy storage	$E^{Bat,\max}$	1000	kWh
	$P^{Bat,ch,\max}$	500	kW
	$P^{Bat,dis,\max}$	500	kW
	$\eta^{Bat,ch}$	0.95	–
	$\eta^{Bat,dis}$	0.95	–
	$\mathrm{SOC}^{Bat,ini}$	0.50	–
	$\mathrm{SOC}^{Bat,ref}$	0.50	–

sis for comparing battery storage and CTES. In the actual optimization, however, the chiller output is calculated using the hourly COP_t^{Ch} profile. Therefore, the comparison should be interpreted as a nominal size-equivalent comparison rather than an exact hour-by-hour equivalence between electrical and cooling storage.

IV. CASE STUDIES

This section applies the proposed PV-supported Cooling Storage Scheduling Framework to compare the operational value of battery energy storage, CTES, and hybrid storage in a grid-connected campus cooling microgrid. The analysis is organized into four cases, as summarized in Table II. Case 1 represents the no-storage reference condition. Case 2 enables only battery energy storage. Case 3 enables only CTES. Case 4 enables both battery energy storage and CTES, with one half of each nominal storage rating adopted in Table I.

Throughout the case studies, the day-ahead EMS model is solved over the same 24-h scheduling horizon and under the same non-cooling electrical demand, PV-generation profile, cooling-demand profile, hourly chiller COP profile, chiller electrical-input limit, grid-import limit, and TOU tariff. Therefore, the differences among the cases are caused only by the available storage configuration. This structure allows the electrical-storage and cooling-storage alternatives to be compared under consistent operating conditions without introducing technology-specific investment assumptions.

The storage ratings in Table II follow the electrical-equivalent normalization defined in the test system parameters. The battery-only and CTES-only cases use the full nominal storage ratings, while the hybrid case uses one half of each nominal rating. Thus, the hybrid configuration combines electrical flexibility and cooling-specific flexibility.

TABLE II
STORAGE CONFIGURATIONS EVALUATED IN THE CASE STUDIES.

Case	Battery Capacity (kWh)	Battery Power (kW)	CTES Capacity (kWh_c)	CTES Power (kW_c)
Case 1: No storage	0	0	0	0
Case 2: Battery only	1000	500	0	0
Case 3: CTES only	0	0	4000	2000
Case 4: Hybrid storage	500	250	2000	1000

A. Case 1: No-Storage Reference Case

In Case 1, no storage device is available, and hence the battery and CTES capacities and power ratings are set to zero, while the chiller serves the cooling demand directly in each hour. The microgrid relies on PV generation and grid import to supply the base electrical demand and the chiller electrical input. Since there is no storage flexibility, PV generation must be used instantaneously by the electrical load or the chiller, while the remaining demand must be supplied by the grid subject to the grid-import limit.

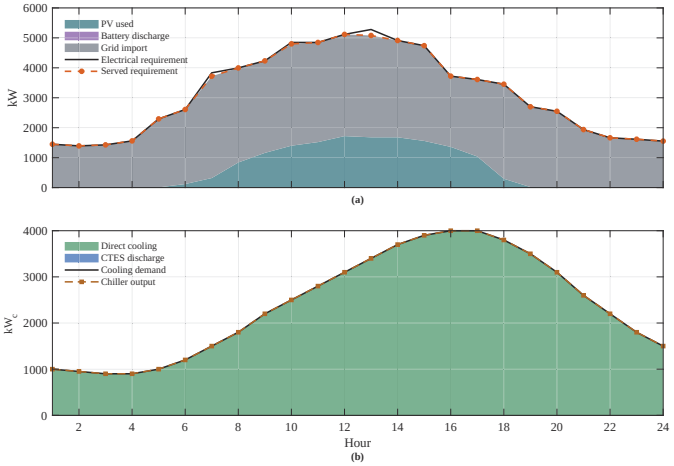

Fig. 2. Hourly operation of Case 1 with no storage: (a) electrical supply and requirement, (b) cooling supply and chiller output.

This case establishes the no-storage reference operation of the PV-supported cooling microgrid. The optimized daily operating cost is \$13,349, of which \$9,738 is associated with grid electricity purchases and \$3,611 is associated with non-cooling electrical load shedding. Although the total shed energy is relatively small compared with the daily base electrical demand, the high shedding penalty makes this component important in the total operating cost.

As shown in Fig. 2(a), grid import is the main supply source over the day. The total grid import energy is 60,264 kWh, and the peak grid import reaches the imposed limit of 3400 kW. The available PV energy is 14,724 kWh and is fully utilized, with no PV curtailment. This indicates that, in the no-storage case, the simultaneous electrical and chiller requirements are sufficient to absorb the available PV generation during daylight hours. However, because no storage is available, PV energy cannot be shifted to later hours or used to relieve grid-constrained periods beyond its instantaneous contribution.

International Journal of Engineering Research & Technology (IJERT)
ISSN: 2278-0181
Vol. 15 Issue 05 , May - 2026

The grid import limit becomes binding during hours 7, 10, and 13, leading to non-cooling load shedding of 113, 48, and 200 kWh, respectively. The total daily load shedding is 361 kWh. The largest shedding occurs during hour 13, when the base electrical demand and chiller electrical input create a total electrical requirement of 5,280 kW, while the available PV generation and the grid-import limit can supply only 5,080 kW. This result shows that the no-storage case is mainly stressed by the coincidence of high electrical demand, cooling-related chiller demand, and the grid import constraint.

Fig. 2(b) shows that the cooling demand is supplied entirely by direct chiller output. The total cooling demand is 57,350 kWh_c, and the corresponding chiller electrical energy is 13,329 kWh. Since no CTES is available, the chiller must follow the hourly cooling demand directly; therefore, the daytime cooling requirement adds to the electrical demand, especially during the hours in which the grid import limit is binding.

Overall, Case 1 has no storage mechanism to shift PV energy, move chiller production away from constrained hours, or support the non-cooling load when the grid-import limit is binding. This limitation provides the reference point for evaluating the storage-based cases that follow.

B. Case 2: Battery-Only Configuration

In Case 2, only the battery energy storage system is enabled with the full nominal rating reported in Table II, while the CTES capacity and power ratings are set to zero. The battery can charge during low-price or high-PV hours and discharge later to reduce grid import during peak-price hours or during hours with limited PV availability.

Since the battery stores electricity, its discharged energy can support either the non-cooling electrical load or the chiller electrical demand, which provides a general electrical-flexibility role within the microgrid.

The optimized daily operating cost in Case 2 is \$9,628, which represents a reduction of \$3,721 compared with the no-storage reference case. This reduction is mainly caused by the elimination of load shedding and by shifting part of the electrical supply from peak price hours to lower price periods through battery charging and discharging.

As shown in Fig. 3(a), the battery changes the electrical supply pattern but does not eliminate the dependence on grid import. The total grid import energy is 60,740 kWh, which is slightly higher than in Case 1. This increase is expected because the battery allows the previously shed load to be served, while its round-trip losses require additional charging energy.

The peak grid import remains equal to the imposed grid limit of 3,400 kW. The battery discharges during grid-constrained and high cost hours, including hours 7, 10, 11, and 13, hence the discharging power reaches the battery limit of 500 kW at hour 13. These discharging actions allow the system to serve the full non-cooling electrical demand without the need for load shedding. Thus, the total non-cooling load shedding is reduced from 361 kWh in Case 1 to zero in Case 2.

Fig. 3(c) shows that the battery is charged mainly during offpeak hours. The charging power reaches 500 kW at hour 4,

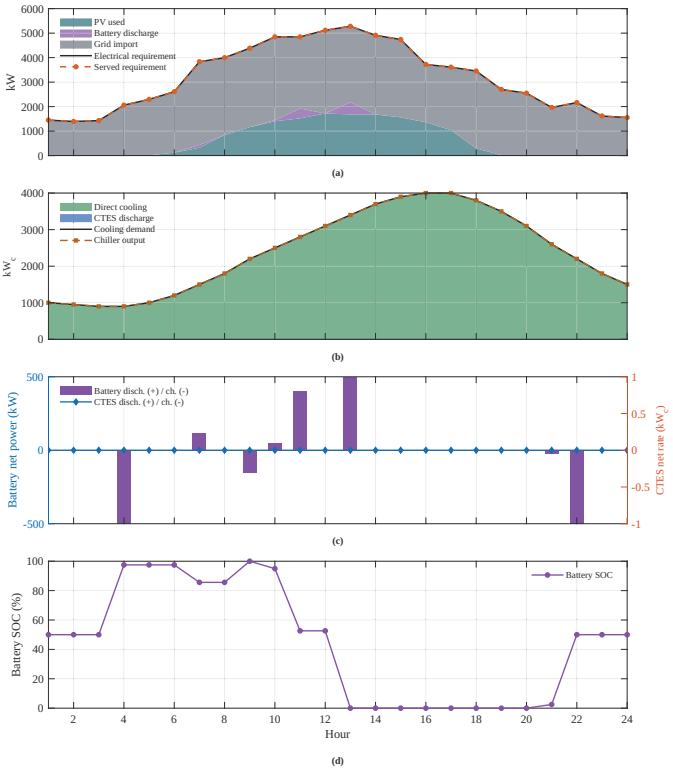

Fig. 3. Hourly operation of Case 2 with battery-only storage: (a) electrical supply and requirement, (b) cooling supply and chiller output, (c) battery charging/discharging rate, and (d) battery state of charge.

while an additional charging action occurs at hour 9 before the peak price period. The battery is also recharged during the late evening, particularly at hours 21 and 22, to satisfy the fixed terminal state-of-charge requirement. Over the day, the battery charging energy is 1,178 kWh and the discharging energy is 1,063 kWh. Fig. 3(d) shows that the battery SOC increases before the peak price interval, decreases during constrained and high cost hours, and returns to the required terminal value of 50% by the end of the day.

The cooling-side operation remains unchanged because CTES is not available in this case. As shown in Fig. 3(b), the cooling demand is supplied entirely by direct chiller output. The total cooling demand and direct cooling supply are both 57,350 kWh_c, and the chiller electrical energy remains 13,329 kWh. Therefore, the battery improves the operation through electrical-side flexibility, while the chiller must still follow the instantaneous cooling demand.

C. Case 3: CTES-Only Configuration

In Case 3, only the CTES tank is enabled, and the CTES unit uses the full nominal rating reported in Table II, while the battery capacity and power ratings are set to zero. In this configuration, the chiller can operate above the instantaneous cooling demand during selected charging hours, particularly when the COP is higher or when grid and tariff conditions are less restrictive, to charge the CTES tank. The stored cooling can then be discharged later to serve part of the cooling demand and reduce chiller operation during peak price or grid-constrained hours.

International Journal of Engineering Research & Technology (IJERT)
ISSN: 2278-0181
Vol. 15 Issue 05 , May - 2026

Unlike battery storage, CTES does not supply the general electrical demand; its flexibility is linked to the cooling demand and the timing of chiller operation. Therefore, this case represents the cooling-storage scenario and shows how storing cooling directly affects chiller scheduling, grid import, load shedding, and operating cost.

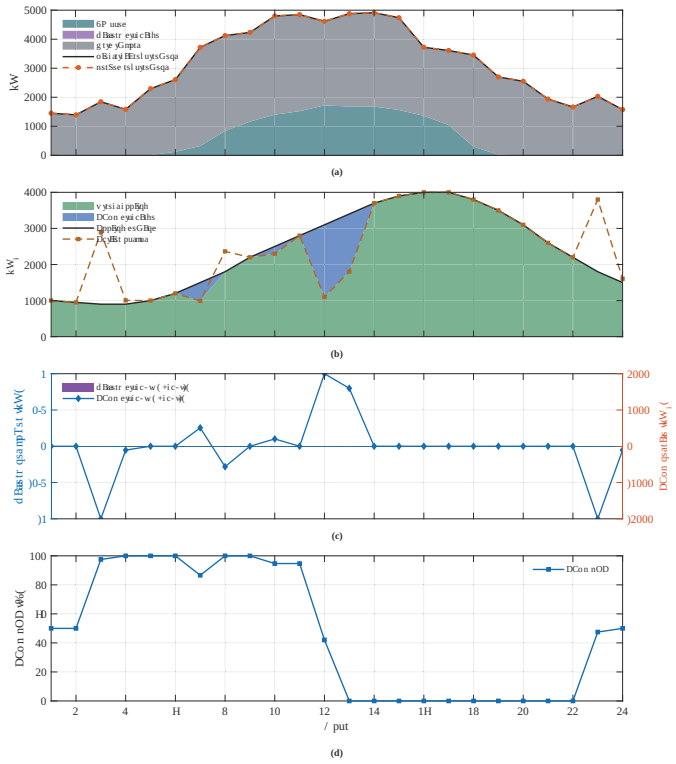

Fig. 4. Hourly operation of Case 3 with CTES-only storage: (a) electrical supply and requirement, (b) cooling supply and chiller output, (c) CTES charging/discharging rate, and (d) CTES stored cooling energy level.

The optimized daily operating cost in Case 3 is \$9,614, which represents a reduction of \$3,735 compared with the no-storage reference case. This reduction is mainly caused by eliminating load shedding and shifting part of the chiller operation away from hours with lower COP values or higher operational stress.

As shown in Fig. 4(a), the CTES changes the electrical operation indirectly by changing the timing of chiller electrical input. The total grid import energy is 60,570 kWh, which is slightly higher than in the no-storage case because the CTES enables full load service and introduces storage losses. The peak grid import remains equal to the imposed limit of 3,400 kW. However, unlike Case 1, no load shedding is required because the CTES reduces chiller input during selected constrained hours.

Fig. 4(b) shows the cooling-side operation in the CTES-only case. Unlike the no-storage case, the chiller output does not have to follow the hourly cooling demand directly. During CTES charging hours, the chiller produces more cooling than the instantaneous demand, while during CTES discharging hours, stored cooling supplies part of the cooling demand and reduces the direct chiller requirement. Over the day, the CTES supplies 4,309 kWh_c of the cooling demand, while the remaining 53,041 kWh_c is supplied directly by the chiller.

Although the total chiller cooling output increases to 57,816 kWh_c because of CTES losses, the chiller electrical energy decreases to 13,274 kWh. This reduction occurs because part of the cooling production is shifted to hours with higher COP values, where the same cooling output requires less electrical input. The operating cost reduction is also supported by the timing of CTES discharge, which reduces chiller electrical input during grid-constrained or high cost hours.

Fig. 4(c) and Fig. 4(d) show the corresponding CTES schedule. The CTES charges mainly during hours 3, 4, 8, 23, and 24, with the largest charging actions reaching the 2,000 kW_c limit. Then, it discharges during hours 7, 10, 12, and 13, where at hour 13, for example, the CTES supplies 1,598 kW_c, reducing the direct chiller cooling requirement and lowering the chiller electrical input to 450 kW. This is important because hour 13 was one of the stressed hours in the no-storage case.

The CTES-only case shows that cooling-specific storage can provide a strong operational benefit even though it cannot directly serve the base electrical demand.

D. Case 4: Hybrid Battery-CTES Configuration

In Case 4, both battery energy storage and CTES are enabled. The hybrid configuration uses one half of the nominal battery rating and one half of the nominal CTES rating reported in Table II.

This case combines two forms of operational flexibility. The battery provides general electrical flexibility because it can support both the non-cooling electrical load and the chiller electrical input. The CTES provides cooling-specific flexibility by shifting cooling production from one period to another. This case therefore shows how the two smaller storage units operate together, providing coordinated operational benefits to the system.

The optimized daily operating cost in Case 4 is \$9,620, which represents a reduction of \$3,729 compared with the no-storage reference case. The hybrid case also eliminates load shedding completely, which indicates that distributing the normalized storage capacity between the two storage technologies is sufficient to remove the grid-constrained shedding, although the smaller rating of each device limits the amount of electrical and cooling shifting.

As shown in Fig. 5(a), grid import remains the main source of electrical supply, but the battery and CTES reduce the electrical stress during selected constrained and high price hours. The total grid import energy is 60,652 kWh, and the peak grid import remains equal to the imposed limit of 3400 kW. The peak grid condition occurs during hours 7 and 10, but no load shedding occurs because the battery discharges during these hours to support the electrical balance.

The battery charging and discharging schedule is shown in Fig. 5(c). The battery charges during hours 6, 8, 19, and 24, while it discharges during hours 7, 10, 11, and 13. The largest battery discharge occurs at hour 13, where the battery

International Journal of Engineering Research & Technology (IJERT)
ISSN: 2278-0181
Vol. 15 Issue 05 , May - 2026

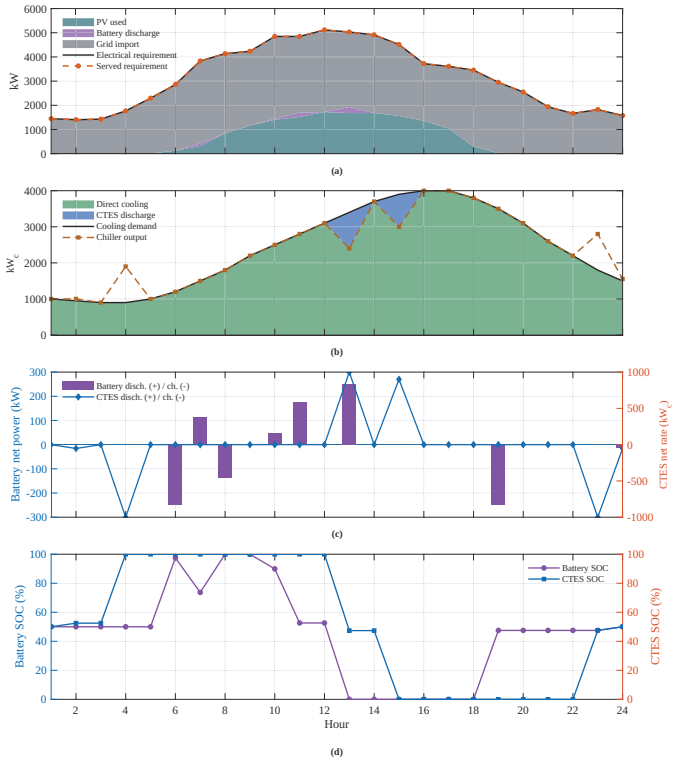

Fig. 5. Hourly operation of Case 4 with hybrid battery-CTES storage: (a) electrical supply and requirement, (b) cooling supply and chiller output, (c) battery and CTES charging/discharging rates, and (d) battery SOC and CTES stored cooling energy level.

reaches its maximum discharging power of 250 kW. The total battery charging energy is 652 kWh, while the total battery discharging energy is 588 kWh.

Fig. 5(d) confirms that the battery is used as a short-term electrical shifting resource. The battery starts at 50% SOC, charges before the peak interval, discharges during grid-constrained hours, and is later restored to the terminal SOC requirement of 50%. The battery reaches its minimum SOC after hour 13 and is later recharged during the evening to satisfy the terminal SOC requirement of 50%.

The CTES operation is coordinated with the battery but acts through the cooling side. As shown in Fig. 5(b), the CTES is charged mainly during off-peak hours and then discharged during the peak-price interval to reduce direct chiller production. The total CTES charging energy is 2105 kWh$_c$, while the total CTES discharging energy is 1900 kWh$_c$. The CTES supplies 1900 kWh$_c$ of the total daily cooling demand, while the remaining cooling demand is supplied directly by the chiller.

The strongest coordination between the two storage devices occurs at hour 13. During this hour, the battery discharges 250 kW and the CTES discharges 1000 kW$_c$. The CTES discharge reduces the chiller cooling output required from 3400 kW$_c$ to 2400 kW$_c$, corresponding to a chiller electrical input of 600 kW. At the same time, the battery supports the electrical balance directly. This combined action allows the system to serve the full electrical demand without load shedding during a stressed peak price hour.

The total chiller electrical energy in the hybrid case is 13,293 kWh, which is lower than in the no-storage and battery-only cases because part of the cooling production is shifted through CTES. However, the reduction is smaller than in the CTES-only case because the hybrid configuration uses only one half of the CTES capacity and power rating. Therefore, the hybrid case provides both electrical and cooling flexibility, but each flexibility pathway is less extensive than in the corresponding full-size single-storage case.

The hybrid case demonstrates that combining battery storage and CTES can remove load shedding while using both electrical and cooling-side flexibility. The battery primarily supports the electrical balance during constrained hours, while the CTES reduces chiller electrical input during selected peak-price hours. This coordinated behavior provides a diversified form of flexibility, even though the half sized ratings limit the maximum shifting contribution of each device.

E. Comparative Discussion

Table III summarizes the main operating indicators for the four storage configurations. The no-storage case has the highest daily operating cost because the grid-import limit causes 361 kWh of non-cooling load shedding. In contrast, all storage configurations eliminate load shedding and reduce the operating cost by about $3,700. This shows that the main value of storage in the studied system is not increasing PV utilization, since PV curtailment is already zero in all cases, nor reducing the observed peak grid import, since the peak remains equal to the imposed grid limit. Instead, the main value is providing operational flexibility during grid-constrained and peak price hours so that the non-cooling electrical demand can be fully served.

TABLE III
SUMMARY OF THE MAIN OPERATING RESULTS FOR THE FOUR CASE STUDIES.

Case	Cost	Grid Energy (kWh)	Load Shedding (kWh)	Chiller Energy (kWh)
Case 1: No storage	$13,349	60,264	361	13,329
Case 2: Battery only	$9,628	60,740	0	13,329
Case 3: CTES only	$9,614	60,570	0	13,274
Case 4: Hybrid storage	$9,620	60,652	0	13,293

Among the storage cases, CTES achieves the lowest operating cost and the lowest chiller electrical energy because it shifts part of the cooling production to hours with higher COP values. However, the cost difference among the three storage cases is small, indicating that all storage configurations provide similar cost benefits under the adopted test conditions. The battery-only case provides general electrical flexibility and eliminates load shedding, but it does not change chiller energy because the cooling demand is still served directly by the chiller. The hybrid case gives a balanced performance close to the best single-storage case, since the battery supports the electrical balance while CTES reduces chiller operation during selected hours.

International Journal of Engineering Research & Technology (IJERT)
ISSN: 2278-0181
Vol. 15 Issue 05 , May - 2026

V. Conclusion

This paper presented a MILP day-ahead scheduling framework for a grid-connected microgrid with PV generation, cooling demand, battery energy storage, and cool thermal energy storage in a hot-climate setting. The model was used to compare no-storage, battery-only, CTES-only, and hybrid battery-CTES configurations under a common set of PV, tariff, demand, chiller, and grid limit assumptions. The hot-climate setting is important because cooling represents a major and time-varying part of the daily demand, and the chiller electrical input depends on the hourly COP.

The results show that storage provides clear operational value under grid-constrained conditions. In the no-storage case, the grid-import limit caused some non-cooling load shedding, leading to the highest daily operating cost. All storage configurations eliminated load shedding and reduced the operating cost. Since PV curtailment was zero in all cases, the main benefit of storage in this test system was not additional PV absorption, but improved operational flexibility during constrained and high-tariff hours.

Among the storage configurations, the CTES-only case achieved the lowest operating cost of because it shifted part of the cooling production to hours with higher COP values and reduced chiller input during selected constrained or high tariff hours. This result highlights the relevance of cooling-side storage in hot climates, where managing when cooling is produced can be as important as managing when electrical energy is stored and discharged.

The battery-only case provided general electrical flexibility, but it did not change the chiller energy because cooling demand was still supplied directly by the chiller. The hybrid case provided a balanced flexibility structure by combining electrical support from the battery with cooling-side shifting from CTES, although its half-sized ratings limited the maximum contribution of each storage pathway.

Overall, the study shows that both battery storage and CTES can improve the operation of PV-supported cooling microgrids, but their benefits occur through different mechanisms. Battery storage supports the electrical balance directly, while CTES reduces chiller loading during selected hours and provides flexibility that is specifically linked to cooling operation in hot-climate systems.

References

[1] E. Alrwishdi, A. AlKassem, S. Al Ahmadi, A. Sadis, A. Draou, M. Ouzzane, and M. Bady, "Energy efficiency and cooling performance of A/C systems in Saudi Arabia's hot climate: A case study," *Measurement: Energy*, vol. 9, Art. no. 100086, 2026.

[2] J. Alshahrani and P. J. Boait, "Reducing high energy demand associated with air-conditioning needs in Saudi Arabia," *Energies*, vol. 12, no. 1, Art. no. 87, 2019.

[3] N. Howarth, N. Odnoletkova, T. Alshehri, A. Almadani, A. Lanza, and T. Patzek, "Staying cool in a warming climate: Temperature, electricity, and air conditioning in Saudi Arabia," *Climate*, vol. 8, no. 1, Art. no. 4, 2020.

[4] A. Zare Ghaleh Seyyedi, M. Gitizadeh, M. Fakhrooeian, and M. Jabareh Nasero, "Achieving the goals of energy arbitrage, peak-shaving, and PV self-consumption using PV-BTM BESS microgrids coupled with a distribution network," *Journal of Energy Storage*, vol. 112, Art. no. 115479, 2025.

[5] S. M. Hasnain, S. H. Alawaji, A. M. Al-Ibrahim, and M.S. Smiai "Prospects of cool thermal storage utilization in Saudi Arabia," *Energy Conversion and Management*, vol. 41, no. 17, pp. 1829–1839, 2000.

[6] J. Vetterli and M. Benz, "Cost-optimal design of an ice-storage cooling system using mixed-integer linear programming techniques under various electricity tariff schemes," *Energy and Buildings*, vol. 49, pp. 226–234, 2012.

[7] T. J. C. Santos, J. M. Torres Farinha, M. Mendes, and J. Monteiro, "Thermal energy storage in renewable energy communities: A state-of-the-art review," *Energies*, vol. 19, no. 5, Art. no. 1363, 2026.

[8] A. V. Olympios, M. Mersch, F. Kourougianni, C. N. Markides, A. M. Pantaleo, A. Kyprianou, and G. E. Georghiou, "A stochastic optimisation framework for integrating photovoltaic systems, heat pumps, and energy storage in buildings," *Applied Thermal Engineering*, vol. 278, Part D, Art. no. 127312, 2025.

[9] J. A. Candanedo, V. R. Dehkordi, and M. Stylianou, "Model-based predictive control of an ice storage device in a building cooling system," *Applied Energy*, vol. 111, pp. 1032–1045, 2013.

[10] F. W. Yu and K. T. Chan, "An alternative approach for the performance rating of air-cooled chillers used in air-conditioned buildings," *Building and Environment*, vol. 41, no. 12, pp. 1723–1730, 2006.

[11] K. Heine, P. C. Tabares-Velasco, and M. Deru, "Design and dispatch optimization of packaged ice storage systems within a connected community," *Applied Energy*, vol. 298, Art. no. 117147, 2021.

[12] C. Tu, Y. Tsai, M. Tsai, and C. Chen, "The optimal operation of ice-storage air-conditioning systems by considering thermal comfort and demand response," *Energies*, vol. 18, no. 10, Art. no. 2427, 2025.

[13] M. Hillen, P. Schönfeldt, P. Groesdonk, and B. Hoffschmidt, "Operational optimization of seasonal ice-storage systems with time-series aggregation," *Energies*, vol. 18, no. 22, Art. no. 5988, 2025.

[14] J. Niu, Z. Tian, Y. Lu, and H. Zhao, "Flexible dispatch of a building energy system using building thermal storage and battery energy storage," *Applied Energy*, vol. 243, pp. 274–289, 2019.

[15] Z. Rostamnezhad, N. Mary, L.-A. Dessaint, and D. Monfet, "Electricity consumption optimization using thermal and battery energy storage systems in buildings," *IEEE Transactions on Smart Grid*, vol. 14, no. 1, pp. 251–265, Jan. 2023.

[16] A. Shakir, J. Zhang, Y. He, and P. Wang, "Coordinated optimization of household air conditioning and battery energy storage systems: Implementation and performance evaluation," *Processes*, vol. 13, no. 3, Art. no. 631, 2025.

[17] J. Kang, J. Wang, C. Liu, S. Ye, and M. Yang, "Coordinated optimization of configuration and operation of a photovoltaic integrated building cooling system with electricity and ice storages under source-load uncertainties," *Energy and Buildings*, vol. 320, Art. no. 114600, 2024.

[18] M. Aldubyan, F. Belaïd, and A. Gasim, "Beyond efficiency gains: Addressing the rebound effect in Saudi Arabian residential cooling," *Development and Sustainability in Economics and Finance*, vol. 1, Art. no. 100007, 2024.

[19] M. Aldubyan, "Future of residential electricity demand in Saudi Arabia and the role of energy efficiency in 2060's net zero pledge," *Development and Sustainability in Economics and Finance*, vol. 8, Art. no. 100086, 2025.

[20] A. Alasiri and M. Nasser, "Comparative analysis of PCM configurations for energy-efficient air conditioning systems: A case study in Riyadh, Saudi Arabia," *Case Studies in Thermal Engineering*, vol. 65, Art. no. 105691, 2025.

[21] W. Matar, "A look at the response of households to time-of-use electricity pricing in Saudi Arabia and its impact on the wider economy," *Energy Strategy Reviews*, vol. 16, pp. 13–23, 2017.

[22] Sh. Mahmoud, Y. Alyousef, Y. Alusaimi, I. Yassin, and A. Alelwan, "Time-of-use tariff program in Saudi Arabia: Design, implementation, and evaluation," *Journal of King Saud University - Engineering Sciences*, vol. 22, no. 2, pp. 165–172, 2010.